JPL PUBLICATION 85-21

ORIGINAL CONTAINS
COLOR ILLUSTRATIONS

# Microwave Hydrology

## A Trilogy

**J.M. Stacey**
**E.J. Johnston**
**M.A. Girard**
Jet Propulsion Laboratory

**H.A. Regusters**
Unicorne Research Foundation




April 1, 1985

National Aeronautics and
Space Administration

**Jet Propulsion Laboratory**
California Institute of Technology
Pasadena, California

JPL PUBLICATION 85-21

# Microwave Hydrology

## A Trilogy

**J.M. Stacey**
**E.J. Johnston**
**M.A. Girard**
Jet Propulsion Laboratory

**H.A. Regusters**
Unicorne Research Foundation

April 1, 1985

National Aeronautics and
Space Administration

**Jet Propulsion Laboratory**
California Institute of Technology
Pasadena, California

The research described in this publication was carried out by the Jet Propulsion Laboratory, California Institute of Technology, under a contract with the National Aeronautics and Space Administration.

## ABSTRACT

Microwave hydrology, as the term is construed in this trilogy, deals with the investigation of important hydrological features on the Earth's surface as they are remotely, and passively, sensed by orbiting microwave receivers. Microwave wavelengths penetrate clouds, foliage, ground cover, and soil, in varying degrees, and reveal the occurrence of standing liquid water on and beneath the surface.

The manifestation of liquid water appearing on or near the surface is reported by a microwave receiver as a signal with a low flux level, or, equivalently, a cold temperature. Actually, the surface of the liquid water reflects the low flux level from the cosmic background into the input terminals of the receiver.

This trilogy describes and shows by microwave flux images:

(1) The hydrological features that sustain Lake Baykal as an extraordinary freshwater resource.

(2) Manifestations of subsurface water in Iran.

(3) The major water features of the Congo Basin, a rain forest.

# FOREWORD

Hydrology is a science that deals with the distribution and circulation of water on the surface of the land, in the soil, and in the underlying rock-forms.

Microwave hydrology is a particular kind of hydrology. As it is conceived here, microwave hydrology is the end product of remote sensing, by microwave sensors, from Earth orbit. It denotes that the waterforms are observed by microwave sensors and connotes that there are advantages in doing so.

Terminology is important. The term "waterforms" denotes liquid water, ice, snow, and permafrost. Particulate water in the atmosphere also affects the distribution and density of waterforms on the surface, and for this reason is included in the family of waterforms that are embraced by hydrology.

Microwave wavelengths penetrate the soils and surface materials of planetary bodies and can, therefore, investigate the occurrence and distribution of the subsurface waterforms. The depth of penetration is controlled by a host of electrical, physical, and chemical factors, mainly the wavelength of the observation and the surface conductivity. In practice, microwaves can penetrate agricultural soils to only a few centimeters, perhaps 10 centimeters as an estimate. In contrast, dry limestone, rock salt, and freshwater iceforms can be penetrated to a depth on the order of tens of centimeters. Glacier ice and very dry snow can be penetrated to the extent of many meters.

The detection and distribution of liquid water on the surface and in the upper layers of the subsurface are perhaps the most reliable and useful measurements of all for microwave sensors. This application is the underlying theme of this trilogy.

The trilogy consists of three independent sections that separately address the occurrence and distribution of waterforms on the surface and in the subsurface of the Earth.

Section 1, Lake Baykal, elucidates a pattern of surface and subsurface water that surrounds and replenishes the lake and establishes the lake's eminence as an extraordinary freshwater resource.

Section 2, Iran, investigates a pattern of subsurface water in Iran that is amply confirmed by visible and infrared sensors.

Section 3, The Congo Basin, describes a rain forest that is observed through a heavy, seemingly inpenetrable, cloud cover. In addition, the headwaters of the Kasai River are identified, and the meandering courses of the Congo (Zaire), Ubangi, and other rivers are clearly shown, even as they widen with overflowing water that causes them to merge with other rivers. Huge swamps are viewed through semi-dense foliage, and subsurface water is identified in the sahel on the perimeter of the Sahara. Lake Chad is surely filled with water, apparently from some underground source. Lake Fitri is full as well.

CONTENTS



Figures

Table

# SECTION 1

# LAKE BAYKAL

## An Extraordinary Freshwater Resource

## A. SUMMARY

Lake Baykal and the hydrological features that surround it have been imaged in color at a microwave wavelength. The length of the image extends from Mongolia to Siberia, and the hydrological features imaged include the Angara River, the watershed area for the Lena River, and numerous surface and subsurface water features.

The image was prepared from the data archive of a microwave receiving system on board an orbiting satellite.

## B. INTRODUCTION

Lake Baykal . . . the deepest lake of all.

It is located in the southern part of eastern Siberia within the Soviet Union, near Mongolia.

Lake Baykal contains 20% of the fresh water on the surface of Planet Earth, and 80% of the fresh water in the Soviet Union. It contains more fresh water than all of the Great Lakes in North America combined.

It is extraordinary indeed. Its length is 636 km, with an average width of 48 km and maximum depth of 1620 meters. The water is clear and the salinity very low. Subsurface features are visible to a depth of 40 meters. There are 27 islands in the lake, and five of these are periodically submerged. Large fish abound, but only one mammal, the Baikal seal. More than 300 rivers and streams, some of which are subsurface, replenish the volume and sustain the lake's level. The Angara River is the only important outlet.

Uncontestedly, Lake Baykal is a major freshwater resource and one of the most significant hydrological features on the surface of the planet. For these reasons, we chose Lake Baykal and the regions that surround it as the subject of our microwave image.

## C. THE MICROWAVE IMAGE

Lake Baykal and its vicinity are shown in Figures 1-1 and 1-2. The color images in Figure 1-2 map the radiant emittances of the surface objects at microwave wavelengths as measured by a collecting aperture in orbit.

The range of the color code is different for the two color images shown. Surface feature contrasts are sometimes seen better with one color code than with another.

Microwave emittances from the surface features are conveyed as relative thermal temperatures which are expressed in shades of blue, green, yellow, and red. Blue shades are cool. Green shades are warmer, then yellow and red.

Open surface water features are shown in blue. Water surfaces reflect the microwave emittances from the cosmic background and the cold atmosphere into the collecting aperture in orbit.

Lake Baykal and the large water features that surround it are blue. The islands in Lake Baykal are purposely suppressed to reduce the dynamic range of the color code that is required to reproduce them.

Green areas are manifestations of swamps and subsurface water near the surface. Green and yellow shades, when patterned as narrow filaments, show rivers and small water features.

Red shades signify dry features such as mountains and deserts. Dense forests appear in shades of red.

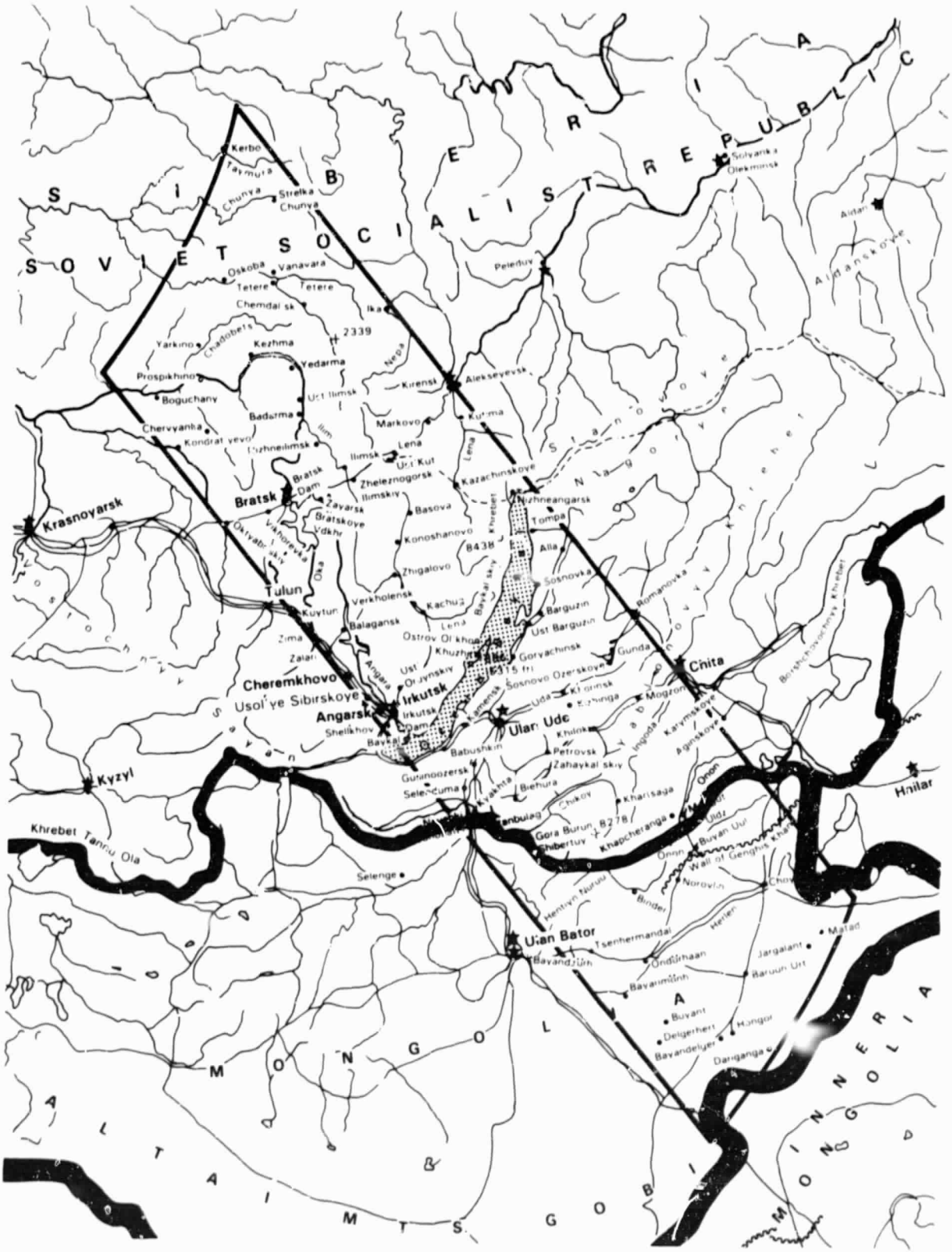


Figure 1-1. Map of the Lake Baykal area

ORIGINAL PAGE
COLOR PHOTOGRAPH

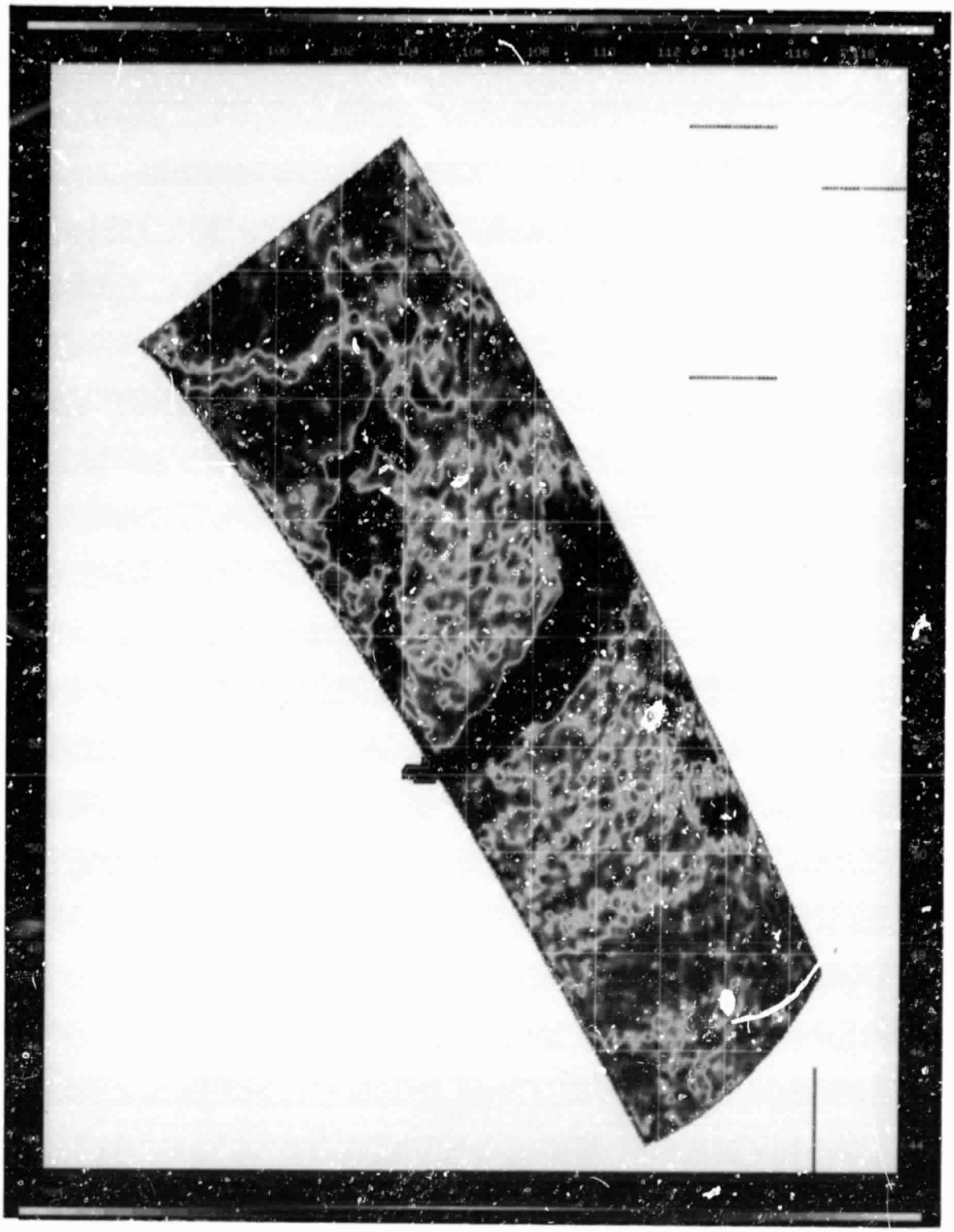

Figure 1-2. Lake Baykal and the hydrological features that surround it: (a) photographed using one color code

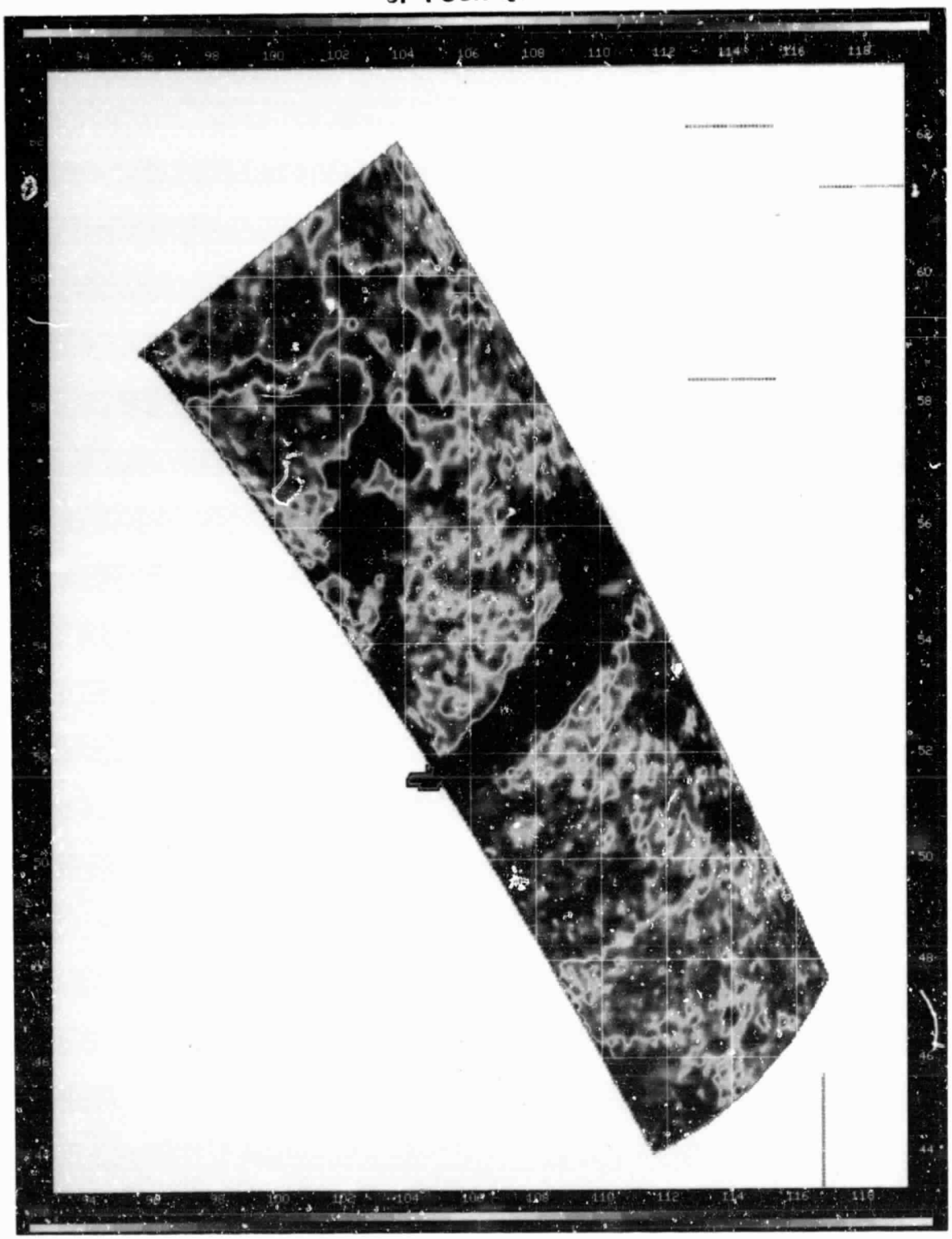

Figure 1-2. Lake Baykal and the hydrological features that surround it: (b) photographed using a slightly different color code to emphasize the occurrence of standing water on the surface by displaying it in deeper shades of blue.

The Angara River emerges from the southwestern perimeter of Lake Baykal; thereafter, it meanders north, then west, and exits the edge of the image. The Angara and the Yenisey converge at Strelka.

The confluence of the Angara and the Ilim Rivers, near 57.5° N lat./ 103° E long., shows outspreading of surface water into flood plains and swamps. Sometimes the outspreading merges with standing pools of precipitation.

The Angara appears to widen intermittently along its course. The apparent widening is caused by the occurrence of conterminous swamps, small tributaries, pools of precipitation, and, occasionally, by the divergence of the main stream due to islands.

The region intervening between the western perimeter of Lake Baykal and Bratsk, with central coordinates 55° N lat./106° E long., is an important watershed area for the Lena River. The many green-yellow patches in the area are indicative of the abundance of standing water on and near the surface.

On the extreme northeast perimeter of Lake Baykal is the delta for the Upper Angara River. The areal extent of the delta is detailed in shades of blue and green.

Near the delta, and to the west, are patches and filaments of green and yellow that are manifestations of small rivers and water areas that contribute to the volume of the lake.

Identifiable lakes and other water features are seen near the eastern perimeter of Lake Baykal, and eastward to the edge of the image.

Southeast of Lake Baykal, in and near Mongolia, there are evidences of many lakes and standing water on the surface and subsurface. These are probably caused by precipitation.

The shades of red at 48° N lat. show drier mountainous terrain.

In the southern extremity of the image, near 45° N lat./112° E long., the shades of blue, green, and yellow are manifestations of swamps and subsurface water in Mongolia, near China.

## D. OBSERVING CONDITIONS

The Lake Baykal image was produced as a color rendering from data taken from the public archive for the passive microwave sensor on the SEASAT spacecraft. The observation occurred on August 2, 1978 at 2220 hours, Universal Time (UT), early morning, local time.

Widespread cumulus cloudforms suffused the image area at the time of the observation. There was no evidence of precipitation.

## E. IMAGE GEOMETRY

The data for the image was collected by an articulating aperture with a surface area of 0.49 $m^2$. The image is a Mercator projection with width and length dimensions of 603 and 1970 km, respectively. The elapsed time for the observation is 5 minutes. The image starts in Mongolia in an ascending node and terminates in Siberia.

## F. DETECTION CRITERIA

The detection capability of the emitting objects on the surface is specified by the flux density (radiant emittance) of a Lambertian Disk Emitter whose diameter is 1600 meters and whose temperature difference, with respect to the Earth's background temperature, is 2 kelvins.

The irradiance of the Lambertian Disk Emitter arrives in the wavefront at the collecting aperture after transiting a slant range of 1000 km. The irradiance is sufficient to produce a 10 dB signal-to-noise ratio.

The signal-to-noise ratio (S/N) is referenced to the phase center of the collecting aperture. The noise term, N, in S/N includes the surface clutter components that enter the directional diagram of the collecting aperture and the RMS noise level of the receiver.

The observing wavelength is 8 mm.

# SECTION 2

# IRAN

## Manifestations of Subsurface Water

## A. SUMMARY

Subsurface water has been detected in Iran by an Earth-orbiting microwave imager. The region of the subsurface water is located in a plateau to the east of the Zagros Mountains.

The source of the subsurface water is the melted snow from the Zagros during the spring and summer months. The runoff water is contained within an underground aqueduct system (to minimize evaporation) and is distributed within the plateau area for irrigation. The region of the subsurface water is near Esfahan.

Two overflights of the spacecraft intersected over the subsurface water area and allowed the microwave imager to observe the phenomenon from two different aspect angles and with a time separation of 11 days.

Visible and infrared images were taken of the subsurface water area (by another spacecraft) that are in close time agreement with the microwave observations. The visible and infrared images show that there is no liquid water on the surface and therefore confirm that the water is in the subsurface, which is penetrated by the microwave sensor.

## B. INTRODUCTION

Once it was called Persia. Today, it is Iran.

It is an expansive land that is characterized by high, rugged, snow-covered mountains that seem to follow the border to the north and to the west. To the south are the Persian Gulf and the Gulf of Oman, near the Arabian Sea. In the middle lies an extensive pattern of high plateaus. (See Figure 2-1.)

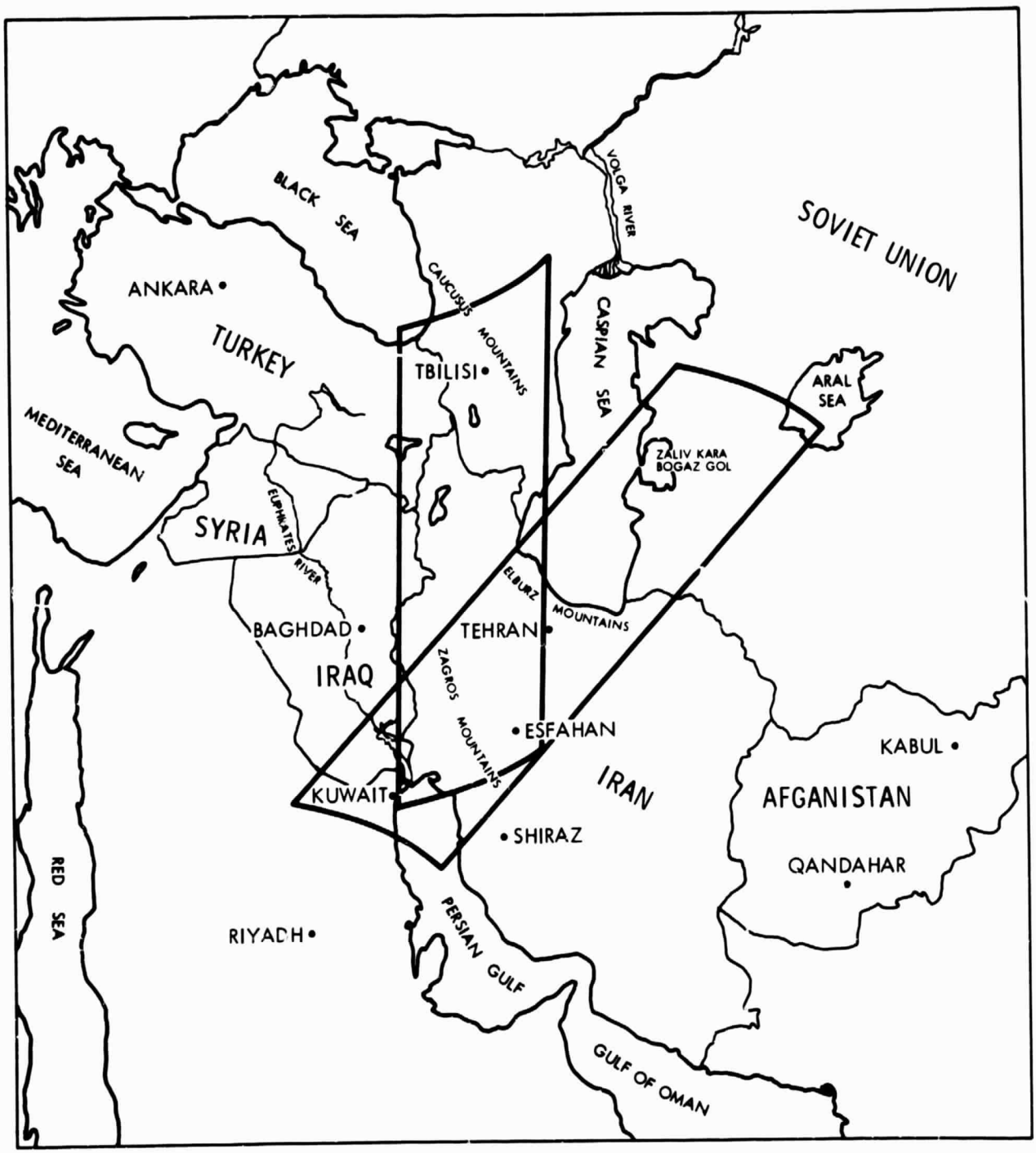


Figure 2-1. Microwave flux image patterns of Iran

The surface of the central plateau is punctuated by an endless and intricate pattern of salt, mud, alkali flats, drift sand, mud basins, and, indeed, some of the most barren and desolate regions on Planet Earth. Occasionally, mountains jut abruptly from the floor of the plateau into the sky to 3000 meters and more.

Iran is bounded on the west by the Zagros Mountains, which sometimes receive more than 1 meter of rainfall during the winter. In the summer, the snow melts and the runoff is captured by a system of underground aqueducts (quanats) that carry the water to the plateau below and distribute it throughout the shallow subsurface for irrigation. The aqueducts are carefully maintained in the subsurface to minimize evaporation.

On the plateau, surface features such as dry lakes, salt lakes, and mud flats appear alternately during the season either as shallow lakes or as parched and cracked basin-like areas that possess no visible manifestations of liquid water. What frequently happens is that the sun evaporates the surface water and, at the same time, dries out the surface of the soil. Immediately below the dry, cracked topsoil may be a layer of liquid water that is shielded from the evaporative effects of the sun. The liquid water level fluctuates near, but below, the visible surface sometimes for long periods of time as it is intermittently replenished by seasonal rains.

Microwave receivers detect subsurface phenomena such as liquid water. The microwave radiation penetrates the visible surface and the top layers of the dry soil to a depth of a few centimeters (a skin depth) and reports the occurrence of water therein.

The manifestations of liquid water both on and within the near surface are reported by a microwave receiver as low flux levels, or, equivalently, as low temperatures.

It is relevant and important to understand that the response of a microwave receiver to the radiation from standing liquid water on or near the surface is very different from that of moist soil where the soil and water have entered into a molecular bond. Liquid water efficiently redirects the very low flux level (low temperature) from the cosmic background into the input port of the receiver. Per contra, moist soil operates as an intrinsic emitter of microwave radiation which produces relatively high flux levels that are interpreted as warm temperatures by the receiver.

Table 2-1 elucidates the expected soil penetration capabilities for microwave wavelengths and for several types of soils and surface features as a function of frequency and surface conductivity. The microwave observations, as described in this report, were taken at 37 GHz (8-mm wavelength). By expectation, and without the benefit of confirming measurements, the penetration depths into agricultural soils for this wavelength may range from 1 to 11 centimeters. Quantitative measurements for soil conductivity, especially in the microwave region, are sparse and a satisfying interpretation of many observations of surface features suffers because of this.

The pattern of the near-surface irrigation water carried by the underground aqueducts in the plateau to the east of the Zagros Mountains, near Esfahan, is the particular subject of this report. The measurements were made by an Earth-orbiting microwave receiver.

## C. THE MICROWAVE FLUX IMAGE

The microwave flux images described here deal with the detection of subsurface water in Iran as it is observed and measured by an orbiting microwave receiver with an articulating antenna system, that is, a microwave imager.

Table 2-1. Penetration Depth (Skin Depth) in Centimeters

| FREQUENCY (GHz) | AGRICULTURAL SENSE | | | DRY LIMESTONE | DRY SANDSTONE | ROCK SALT | MARINE SAND | CONNATE WATER (IN ROCKS) | ARIZONA SOIL | AUSTIN, TEXAS SOIL (VERY DRY) |
|---|---|---|---|---|---|---|---|---|---|---|
| | GOOD SOIL | AVERAGE SOIL | POOR SOIL | | | | | | | |
| 6.633 | 2.6 | 8.3 | 26.4 | 87.4 | 61.8 | 87.4 | 0.83 | 0.87 | 1.95 | 7.18 |
| 10.69 | 2.0 | 6.6 | 20.8 | 68.8 | 48.7 | 68.8 | 0.66 | 0.69 | 1.54 | 5.66 |
| 18.0 | 1.6 | 5.1 | 16.0 | 53.1 | 37.5 | 53.1 | 0.51 | 0.53 | 1.19 | 4.36 |
| 21.0 | 1.5 | 4.7 | 14.8 | 49.1 | 34.7 | 49.1 | 0.47 | 0.49 | 1.11 | 4.04 |
| 37.0 | 1.1 | 3.5 | 11.2 | 37.0 | 26.2 | 37.0 | 0.35 | 0.37 | 0.83 | 3.04 |

| FREQUENCY (GHz) | GLACIER ICE | FRESH WATER ICE | SEA ICE | PERMAFROST | SNOW (DRIFTED, WET) | SEAWATER | FRESH WATER |
|---|---|---|---|---|---|---|---|
| 6.633 | 663 | 195 | 21.4 | 87.3 | 113 | 0.29 | 26.4 |
| 10.69 | 487 | 154 | 16.9 | 68.8 | 88.9 | 0.23 | 20.8 |
| 18.0 | 375 | 119 | 13.0 | 53.1 | 68.5 | 0.18 | 16.0 |
| 21.0 | 347 | 110 | 12.0 | 49.1 | 63.4 | 0.16 | 14.8 |
| 37.0 | 262 | 83 | 9.1 | 37.0 | 47.8 | 0.12 | 11.2 |

NOMINAL VALUES OF SURFACE CONDUCTIVITY IN MHOS/METER*

| | | | |
|---|---|---|---|
| • GOOD SOIL | 0.055 | • GLACIER ICE | 1E-06 |
| • AVERAGE SOIL | 0.0055 | • FRESH WATER ICE | 1E-05 |
| • POOR SOIL | 0.00055 | • SEA ICE (-40 C) | 8.33E-04 |
| • DRY LIMESTONE | 5E-05 | • PERMAFROST | 5E-05 |
| • DRY SANDSTONE | 1E-04 | • SNOW (DRIFTED, WET) | 3E-05 |
| • ROCK SALT | 5E-05 | • SEAWATER | 4.5 |
| • MARINE SAND | 0.55 | • FRESH WATER | 5.5E-04 |
| • (CONNATE WATER IN ROCKS) | 0.5 | | |
| • ARIZONA SOIL | 0.1 | | |
| • AUSTIN, TEXAS SOIL (DRY) | 0.0074 | | |

*SURFACE CONDUCTIVITY VARIES WIDELY WITH FREQUENCY, TEMPERATURE, WATER CONTENT, IMPURITIES... AND OTHER FACTORS. THE VALUES GIVEN FOR SURFACE CONDUCTIVITY ARE ADOPTED FOR PLANNING PURPOSES OR FOR GENERAL INTEREST. MAINLY, THEY ARE BASED ON LOW-FREQUENCY MEASUREMENTS < 100 KHz, OR ARE DERIVED FROM CASUAL EXTRAPOLATIONS AT MICROWAVE WAVELENGTHS.

The flux images are displayed in color in Figures 2-2 and 2-3, and are keyed to the bold black rectangles shown in Figure 2-1.

The subsurface water is observed in the plateau region immediately to the east of the Zagros Mountains. The irregular pattern of the subsurface water runs generally northwest to southeast and includes Esfahan.

The shades of blue and green, intervening between 34° N lat./50° E long. and 32° N lat./52° E long., describe the approximate geographical extent of the subsurface water as it is displayed in the images. Actually, the subsurface water extends beyond the border of the images to the southeast.

The width of the subsurface water pattern is approximately 150 km at its widest point; the length exceeds 500 km, as it is shown in the image.

The color code for the images is based on relative flux magnitudes. Low flux levels are expressed by shades of blue. The highest flux levels are expressed by shades of pink.

Microwave flux levels may also be expressed as thermodynamic temperatures where colder temperatures appear in shades of blue and higher temperatures appear in shades of pink. Thermodynamic temperatures are linearly related to flux magnitudes and they may change instantaneously, the same as the flux. Per contra, thermometric temperatures are construed as real temperatures that, in context, are measured by mercury-bulb thermometers, as an example. The color images in this report are best interpreted as relative flux.

The color code expresses increasing flux intensities in shades of blue, green, yellow, red, and pink as shown from left to right below:

PINK

RED

YELLOW

GREEN

BLUE

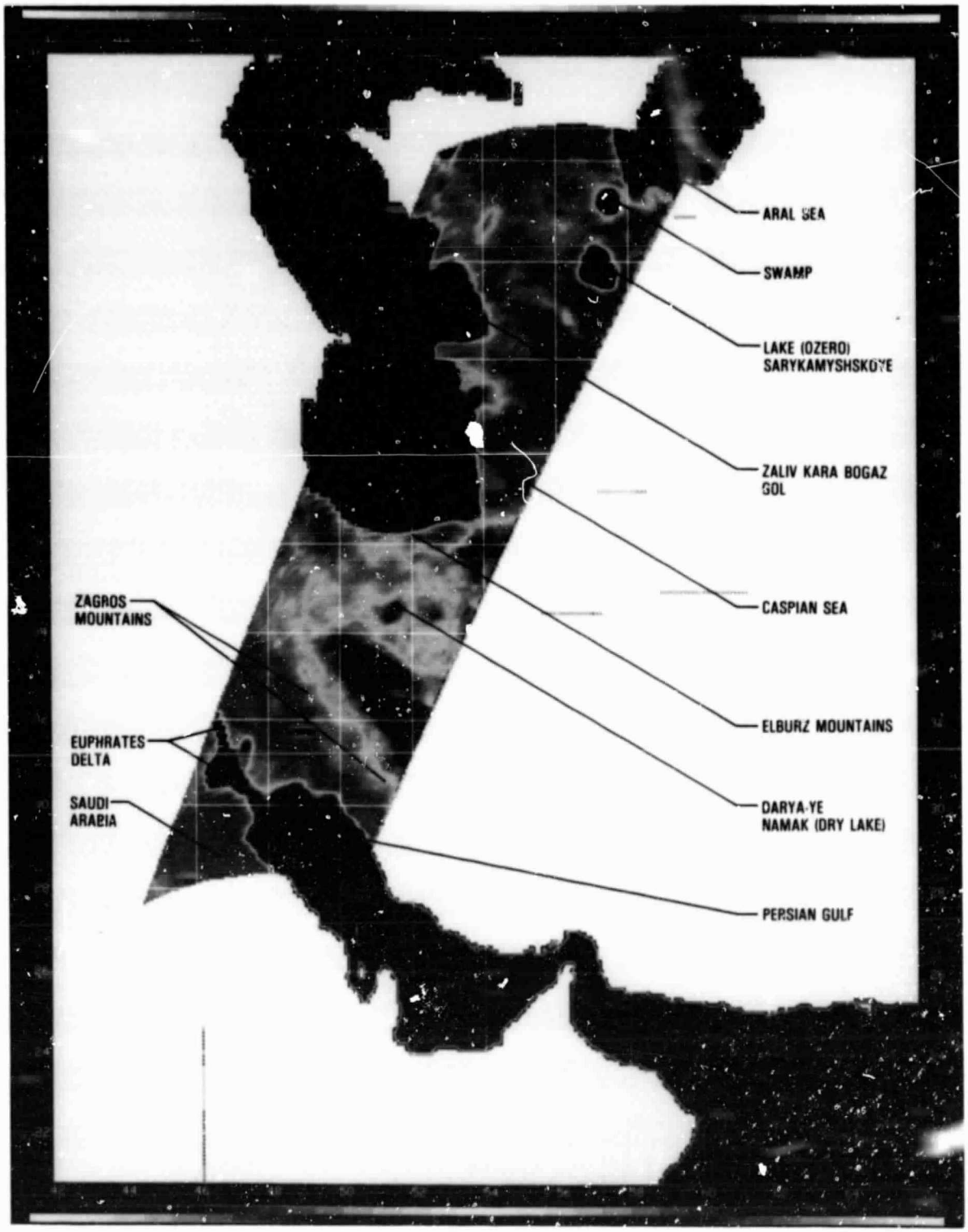


Figure 2-2. Annotated flux image of the Aral Sea to the Persian Gulf

ORIGINAL PAGE
COLOR PHOTOGRAPH

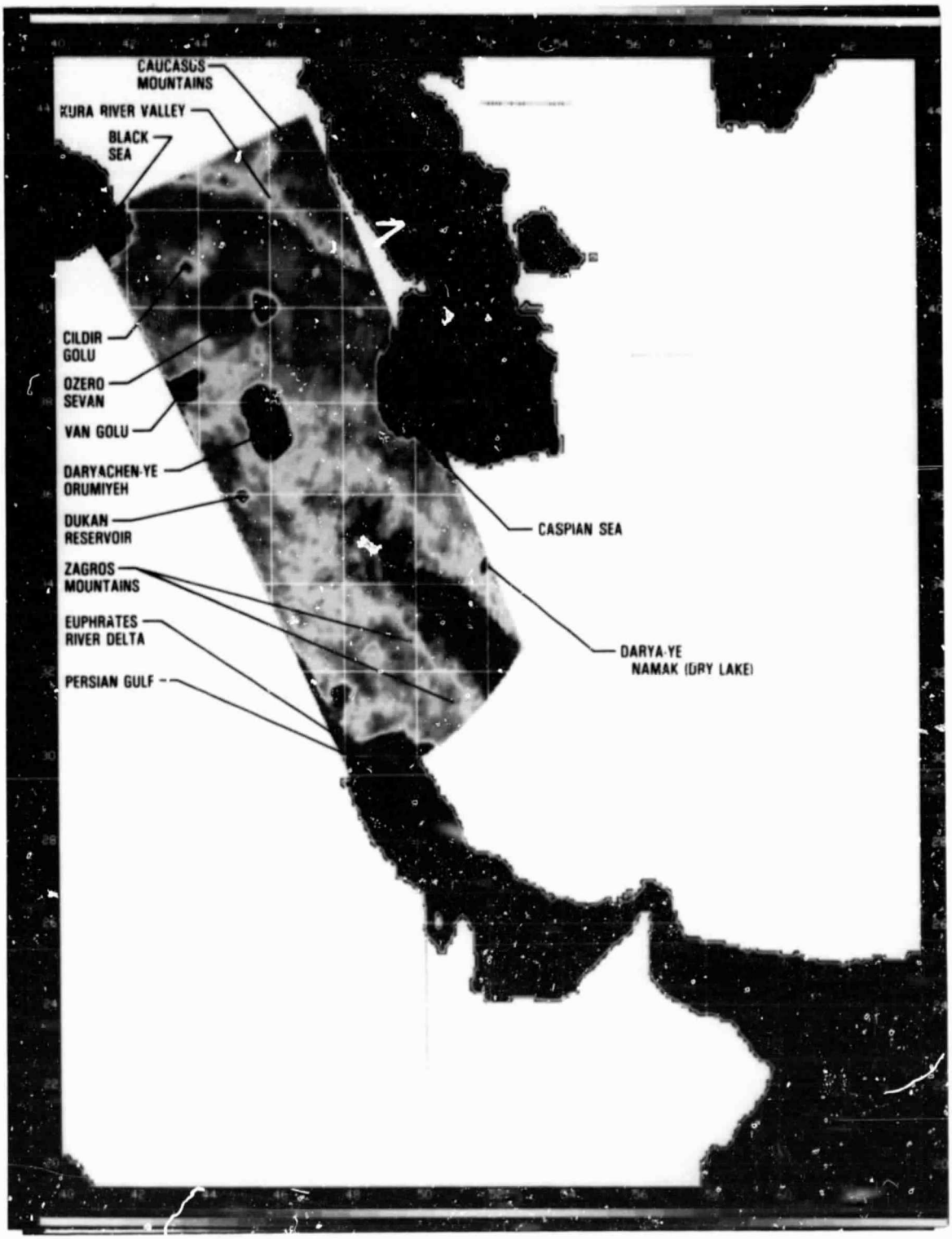


Figure 2-3. Annotated flux image of the Persian Gulf to the Black Sea

Standing water on the surface, lakes, and seawater are represented by blue shades. Surface and subsurface liquid water operates to redirect the extremely low flux level that arrives from the cosmic background into the input ports of the receiver. Thermodynamically, when water occurs within a skin depth of the visible surface, it appears cold.

Mountains, dry plateau areas, and deserts appear as warm, emitting surface regions and are shown in shades of red and pink.

Transition regions that occur between water features and mountains (or deserts) appear in shades of green and yellow.

Two intersecting orbital overflight patterns are outlined in bold black borders in Figure 2-1 and again as corresponding color renderings in Figures 2-2 and 2-3. These rectangular patterns represent the area scanned by an articulating antenna system as viewed from an orbiting spacecraft.

Figure 2-2 originates over the Aral Sea (in the Soviet Union) and terminates in Saudi Arabia. Figure 2-3 originates in Iran (near the northern extremity of the Persian Gulf) and terminates in the Soviet Union between the Black Sea and the Caspian Sea. The two images intersect in the region of the subsurface water near 32° N lat./52° E long., east of the Zagros Mountains.

The color images are annotated and clearly identify some of the principal water and surface features within the Soviet Union, Iran, and Turkey.

Figure 2-2 was taken during an overflight on July 11, 1978, at 1434 hours Universal Time (UT). Earlier in the same day (0741 hours UT), visible and infrared images (Figures 2-4 and 2-5) were taken by another spacecraft whose land coverage included the total area of the overflight shown by the color image. The visible and infrared images show no manifestations of surface water in the region east of the Zagros Mountains. The liquid water surfaces of numerous small lakes and other water features appear in abundance in the

Figure 2-4. A visible-sensor image taken on July 11, 1978, at 0741 hours UT. This visible image, which is centered on the Mesopotamia area (Syria, Iraq, and Kuwait), shows the Aral Sea, Caspian Sea, Persian Gulf, Black Sea, eastern Mediterranean Sea, and Red Sea (see Figure 2-5 for the infrared-sensor image of the same area). The Tigris and Euphrates delta extends northwesterly from the Persian Gulf. The Zagros Mountains run northwest to southeast along the eastern shore of the Persian Gulf and extend along the eastern edge of the Tigris and Euphrates delta.

The white patches in the image are cumulus/stratus cloudforms that cover the eastern end of the Black Sea, the southern extremity of the Red Sea, the Gulf of Oman, and a portion of the Arabian Sea. Surface water features such as seas, lakes, and rivers appear in the image as dark patches and filaments, while land features appear in lighter shades. Notably, there is no evidence of extended standing water patterns on the surface in the region to the east of the Zagros Mountains. (Photograph produced from the U.S. Department of the Air Force (USAF) Defense Meteorological Satellite Program (DMSP) film transparencies archived for the National Oceanic and Atmospheric Administration (NOAA)/National Environmental Satellite Data and Information Center (NESDIS) at the University of Colorado, Cooperative Institute for Research in Environmental Sciences (CIRES)/National Snow and Ice Data Center)

ORIGINAL PAGE
COLOR PHOTOGRAPH

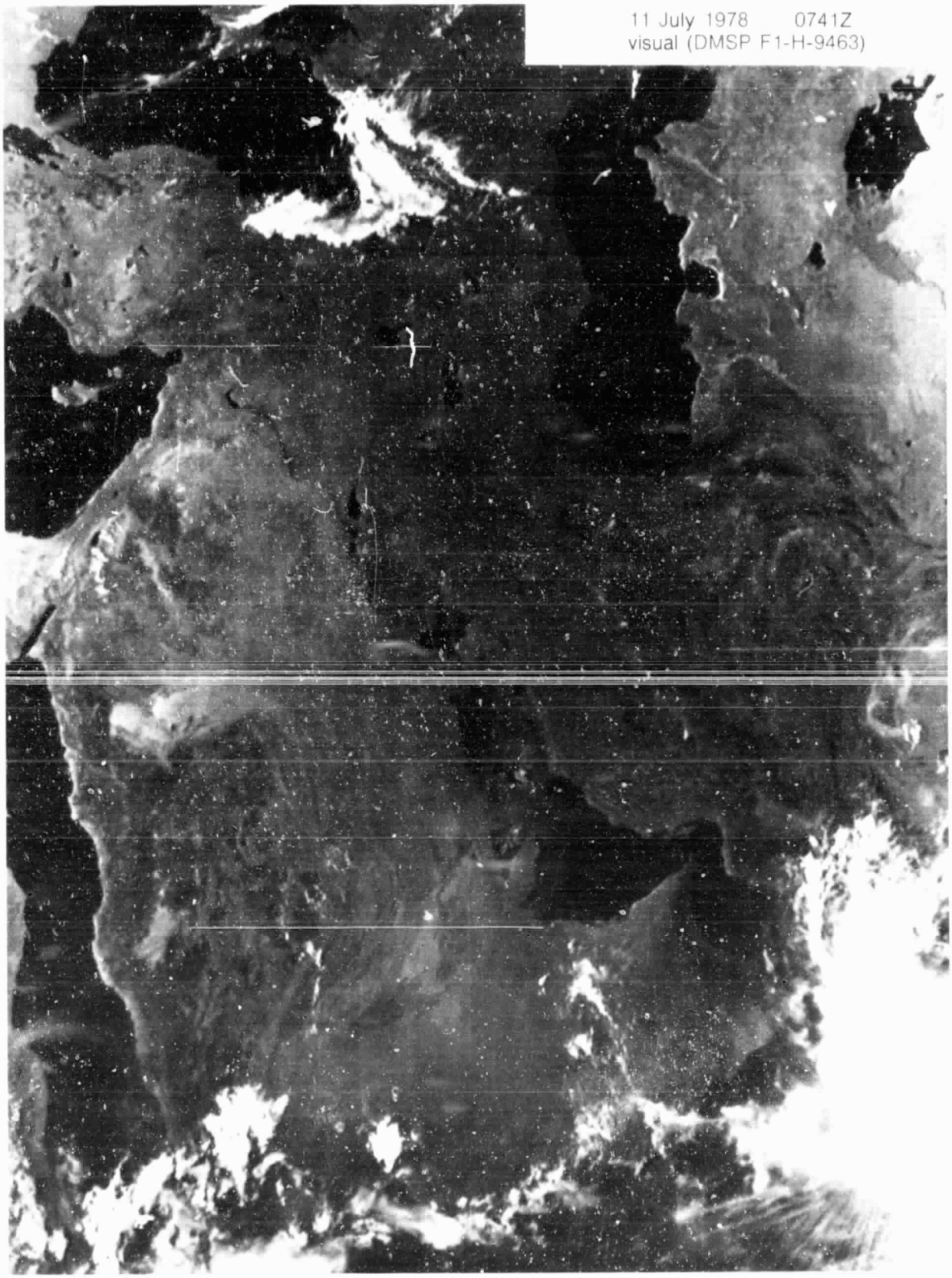

11 July 1978 0741Z
visual (DMSP F1-H-9463)

ORIGINAL PAGE
COLOR PHOTOGRAPH

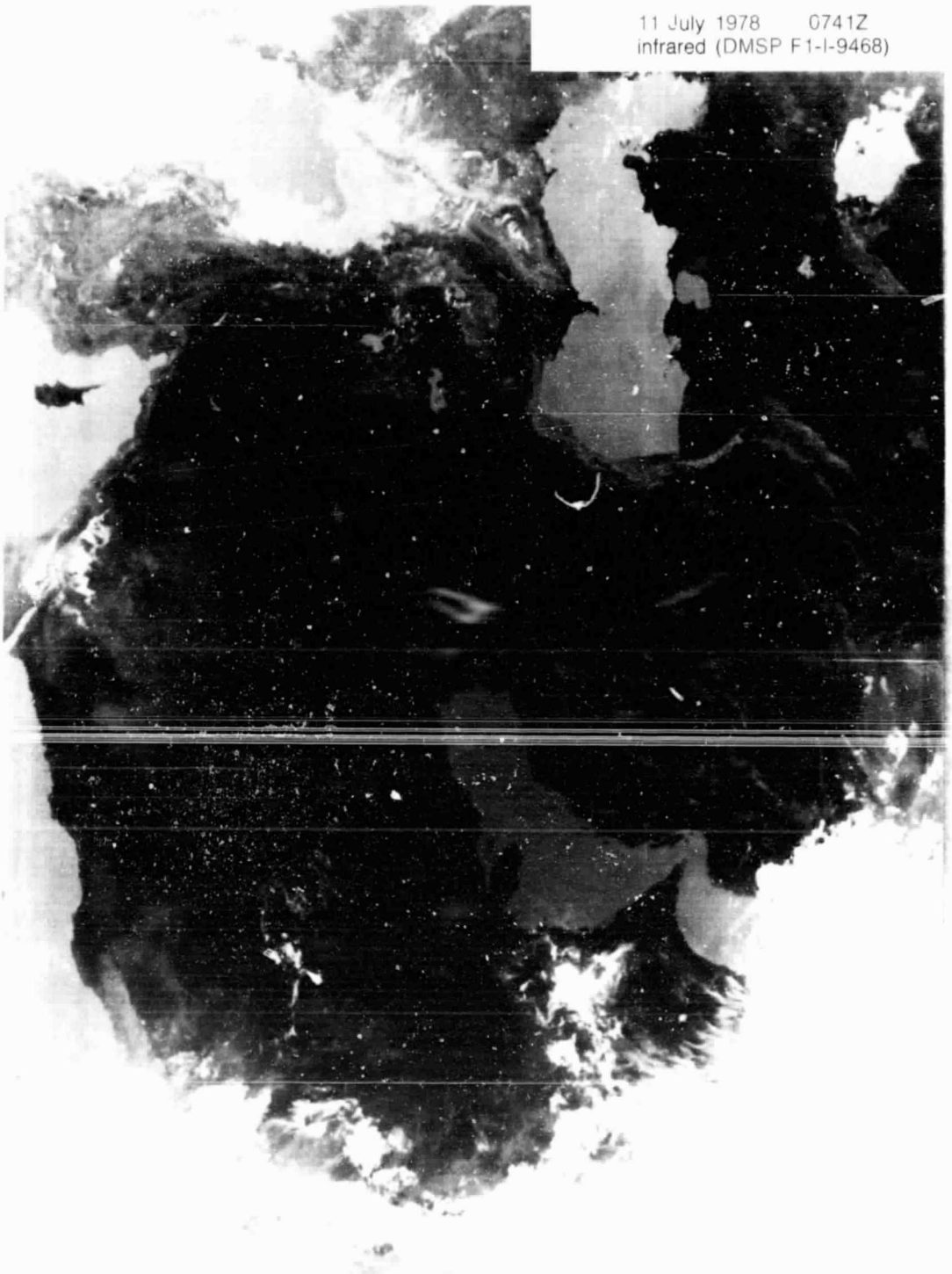


Figure 2-5. An infrared-sensor image taken on July 11, 1978, at 0741 hours UT. This image shows the same area as that in Figure 2-4 and was taken at the same time. (Photograph produced from the USAF DMSP film transparencies archived for NOAA/NESDIS at the University of Colorado, CIRES/National Snow and Ice Data Center)

visible and infrared images, but there is no evidence of standing water on the surface in the plateau region to the east of the Zagros. It is the soil-penetrating capability of microwave wavelengths that is needed to identify subsurface liquid water.

Figure 2-3 was taken during an overflight on July 22, 1978 (eleven days later), at 0218 hours UT. Later in the same day, at 0748 hours UT, visible and infrared images (Figures 2-6 and 2-7) were taken by another spacecraft whose coverage included the total area of the overflight shown in the corresponding color image. Again, there are no manifestations of standing water on the surface in the plateau region to the east of the Zagros.

It is important to compare the pattern of the subsurface water in the region near Esfahan, and near $32^{\circ}$ N lat./$52^{\circ}$ E. long., for the two images. Figure 2-3 shows a different detailed distribution of the subsurface water than Figure 2-2. This is expected: the aspect angles are different and there is an 11-day lapse in time between the two images. Presumably, the distribution of the subsurface water could also change during this period of time.

The aspect angle is an important criterion as it affects observations of land surfaces. Surface areas appear differently when viewed from another direction. Subsurface water cells, for example, have an irregular, three-dimensional geometry. For this reason alone, the water cells appear differently with respect to the aspect angle. In addition, there are the effects of variable shadowing of the water cells caused by hills, mountains, foliage, and ground cover, which, in the main, operate to produce variable attenuation in the slant path between the subsurface water and the microwave imager.

Figure 2-6. A visible-sensor image taken on July 22, 1978, at 0748 hours UT. This visible image, which is centered on the Mesopotamia area (Syria, Iraq, and Kuwait), shows the Aral Sea, Caspian Sea, Persian Gulf, Black Sea, eastern Mediterranean Sea, and Red Sea (see Figure 2-7 for the infrared-sensor image of the same area). The Tigris and Euphrates delta extends northwesterly from the Persian Gulf. The Zagros Mountains run northwest to southeast along the eastern shore of the Persian Gulf and extend along the eastern edge of the Tigris and Euphrates delta.

The white patches in the image are cumulus/stratus cloudforms that cover the western end of the Black Sea, the northern end of the Caspian Sea, and the southern part of the Red Sea. Surface water features such as seas, lakes, and rivers appear in the image as dark patches and filaments, while land features appear in lighter shades. Notably, there is no evidence of extended standing water patterns on the surface in the region to the east of the Zagros Mountains. (Photograph produced from the USAF DMSP film transparencies archived for NOAA/NESDIS at the University of Colorado, CIRES/National Snow and Ice Data Center)

ORIGINAL PAGE
COLOR PHOTOGRAPH

22 July 1978 0748Z
visual (DMSP F1-H-9624)

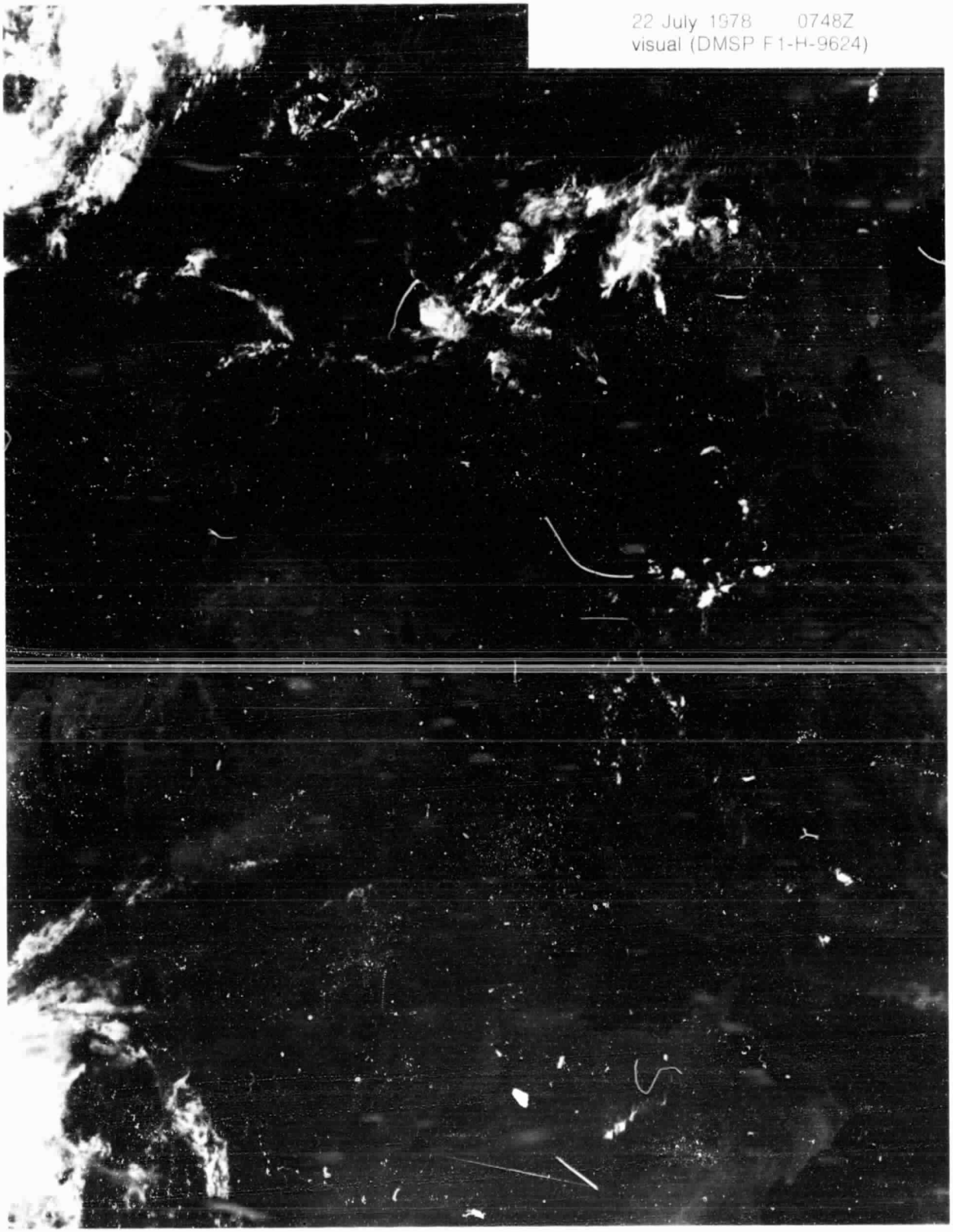

ORIGINAL PAGE
COLOR PHOTOGRAPH

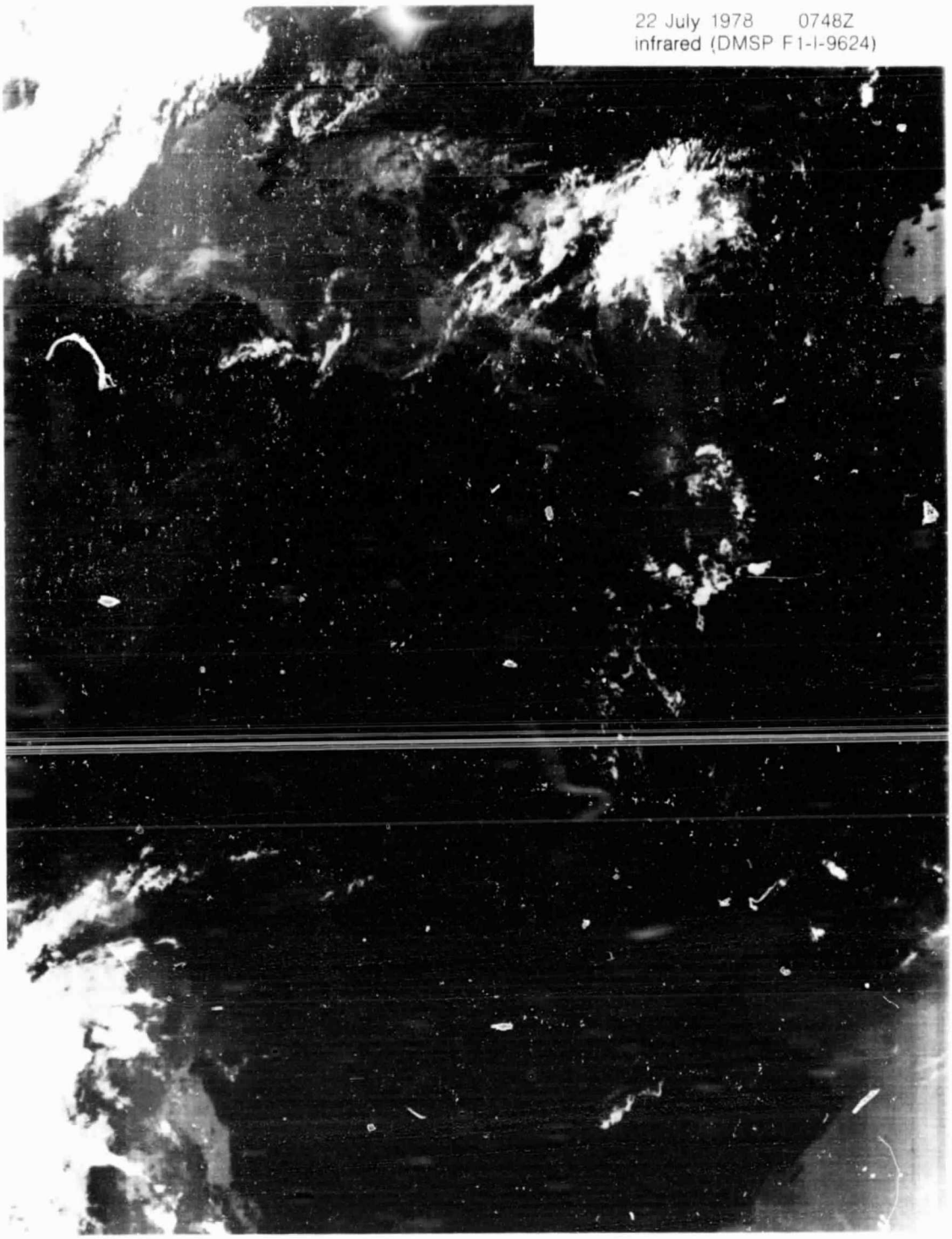


Figure 2-7. An infrared-sensor image taken on July 22, 1978, at 0748 hours UT. This image shows the same area as that in Figure 2-6 and was taken at the same time. (Photograph produced from the USAF DMSP film transparencies archived for NOAA/NESDIS at the University of Colorado, CIRES/National Snow and Ice Data Center)

The differences in the detailed distribution of the subsurface water that are separately caused by the aspect angle and by the 11-day elapsed time interval between the overflights are not reconcilable because there are too many unknown factors to reckon with. Suffice it to say that these distribution differences are expected, though as yet no quantitative determinations can be made about whether the differences were caused by the aspect angle or the elasped time, because of lack of experience--and lack of confirming surface truth.

## D. DETECTION CRITERIA

The detection capability of the microwave imager, for emitting objects on the surface, is specified by the flux density (radiant emittance) of a Lambertian Disk Emitter whose diameter is 1600 meters and whose temperature difference, with respect to the Earth's background temperature, is 2 kelvins.

The irradiance of the Lambertian Disk Emitter arrives in the wavefront at the collecting aperture after transiting a slant range of 1000 km. The irradiance is sufficient to produce a 10-dB signal-to-noise ratio (S/N). The S/N is referenced to the phase center of the collecting aperture. The noise term, N, in S/N includes the surface clutter components that enter the directional diagram of the collecting aperture and the RMS noise level of the receiver.[1]

The observations were taken by the microwave imager on the SEASAT spacecraft. The articulating aperture for the imager has a collection area of 0.49 m. The observing wavelength was 8 millimeters.

The data for the observations were taken from a public archive for the microwave sensor.

---

[1] J. M. Stacey, "Power Transfer from Natural Emitters to Collecting Apertures at Microwave Wavelengths," JPL Publication 84-48, Jet Propulsion Laboratory, Pasadena, California, December 1, 1984.

# SECTION 3

# THE CONGO BASIN

## A Rain Forest

## A. SUMMARY

The most prominent and interesting features of the Congo Basin are imaged passively by microwaves. The persisting cloud canopy over the basin can thus be penetrated over a wide region to reveal the major rivers, lakes, swamps, and features of the adjacent desert area.

The microwave flux image is presented as a color rendering to better illustrate the subtle characteristics of the features in the basin and to show their areal distributions.

## B. INTRODUCTION

The Congo Basin, the rain forest: that portion of Africa, mainly in Zaire, that generously straddles the equator. To the north it touches Lake Chad and the Sahara, and to the east it merges with the savannahs near Lake Tanganyika and Lake Victoria.

It is a basin in the literal sense of the word, a place to travel in small boats, bare feet, or hip boots. Dry spots that are suitable for resting or taking food occur infrequently, and when they do, they are generally atop the protruding roots of an overturned tree.

Dry land is a curiosity.

The treetops overlap and interlock, forbidding visible, infrared, and sometimes microwave penetration. Where there are gaps in the dense, intertwined foilage, we see swamps populated by floating debris, tree stumps, matted grasses, and billions of leaves, branches, and scum.

Mostly, it is a place of beauty: the greenest greens, the bluest blues, enormous flowers and gaudy floral displays, optically smooth lakes and waterways that mirror everything in sight. Even the persisting clouds are beautiful.

The sky is wet, the trees are wet, and the basin floor is wet with standing water everywhere. It is all explainable, though: the basin is a rain forest with more than 2 meters of rainfall annually.

Typically, the skies are filled with clouds--raining clouds, clouds of all kinds--as well as haze, mist, and fog. Each phenomenon in its own way forbids the penetration of short wavelengths.

For all of this, we despair with the propagation limitations of the visible and the infrared, and turn to the comparative excellence of the microwave flux image to penetrate, map, and explain some of the more prominent and interesting features of the basin.

## C. THE MICROWAVE FLUX IMAGE

The region covered by the microwave flux image is illustrated in Figure 3-1. The image commences in southern Zaire and passes northwestward over portions of the Central African Republic, Cameroon, Nigeria, and Chad, terminating at the fringe of the Sahara (sahel) near Lake Chad.

The microwave flux image, Figure 3-2, is displayed in 40 colors: 10 shades each of blue, green, yellow, and red. Blue shades show areas of open water, such as rivers, or swamps with little or no foliage. Green shades depict areas with standing water on the surface as viewed through light foliage. Mixed shades of blue and green sometimes identify a pattern of small streams that are tightly braided together. Yellow shades identify features that seem to change their character seasonally, such as intermittent swamps, foliage on higher ground, denser foliage, and areas heavily shrouded by grass. Red shades identify features that occur in the transition region extending from the basin to the dry lakes, lava beds, and sands of the sahel.

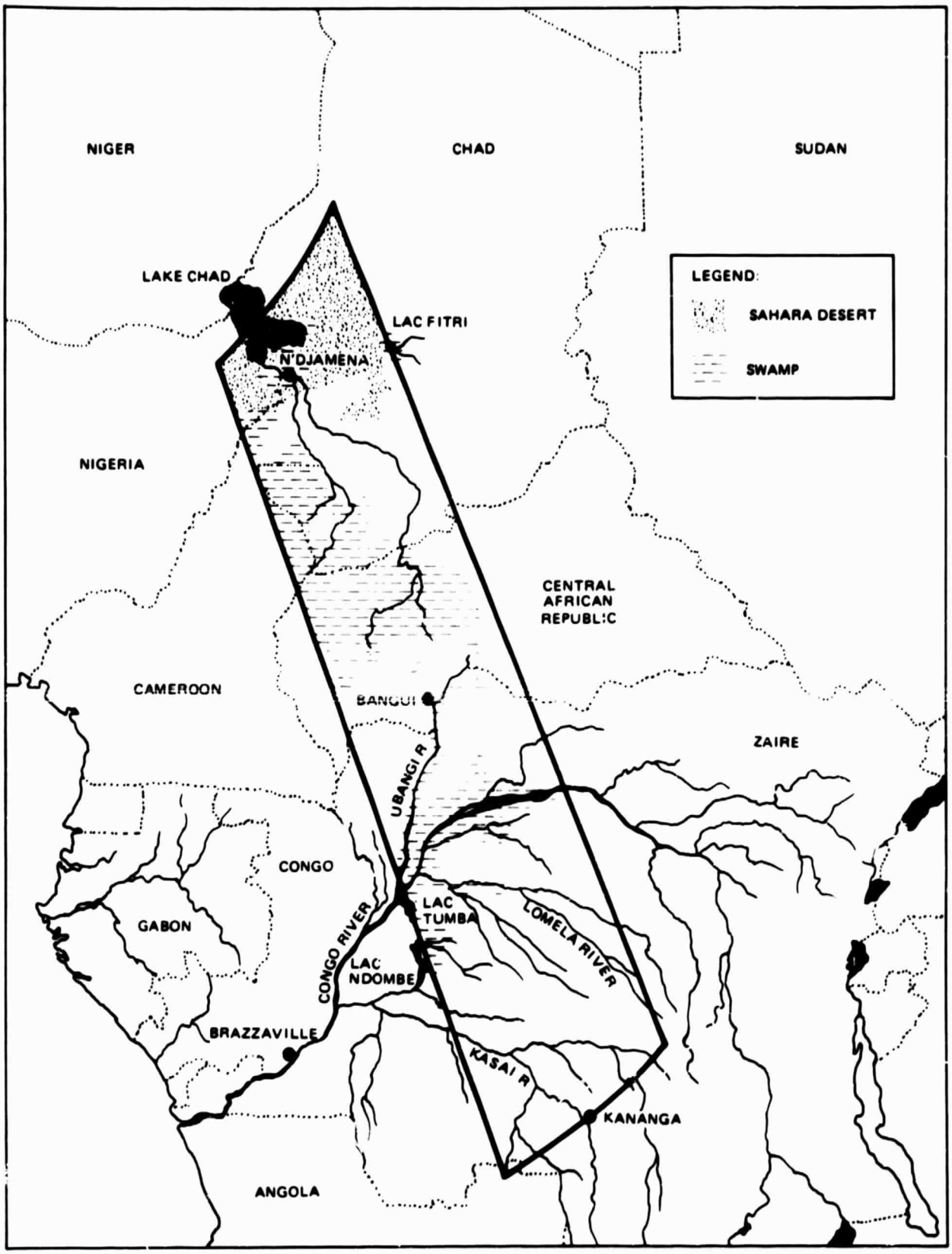


Figure 3-1. The Congo Basin, the heart of Africa

Figure 3-2. A microwave flux image of the Congo Basin

The microwave flux image of Figure 3-2 is annotated in Figure 3-3.

The microwave flux imager measures the power, in units of watts, that is emitted by land phenomena. The features of the images are interpreted from the relative flux patterns.

The geographical coordinates for the image are expressed in degrees of latitude (vertical scale) and longitude (horizontal scale). Because the image extends onto both sides of the equator, degrees of latitude for the southern hemisphere are preceded by a minus sign.

At the extreme lower portion of the image, near $7^{\circ}$ S lat./$21^{\circ}$ E long., is the headwater (watershed) region of the Kasai River. The intermittent patterns of blue, green, and yellow that finally seem to converge into the Kasai are braided streams and pools of standing water that are sometimes viewed through the variable density of the foliage. The main bore of the Kasai exits the image near $3.5^{\circ}$ S lat./$18^{\circ}$ E long. The Kasai is a tributary of the Congo.

The Congo River is shown as a curved blue ribbon that passes across the width of the image near the center. It exits the image near $2^{\circ}$ N lat./$22^{\circ}$ E long. (In the eastern segment of this ribbon appears a modulated pattern in the sides of the river. It is a software imperfection and should be ignored.)

At the confluence of the Congo and the Ubangi, near $0^{\circ}$ lat./$18^{\circ}$ E long., is a large area of small streams and pools of standing water that interconnect the two rivers. The Congo and the Ubangi converge near Lake Tumba ($1^{\circ}$ S lat./$18^{\circ}$ E long.). The Ubangi forms a long political boundary between Zaire and the Central African Republic.

Lake Tumba appears as an extension to the sides of the Congo because of the interconnecting surface waters that are viewed by the imager through the foliage.

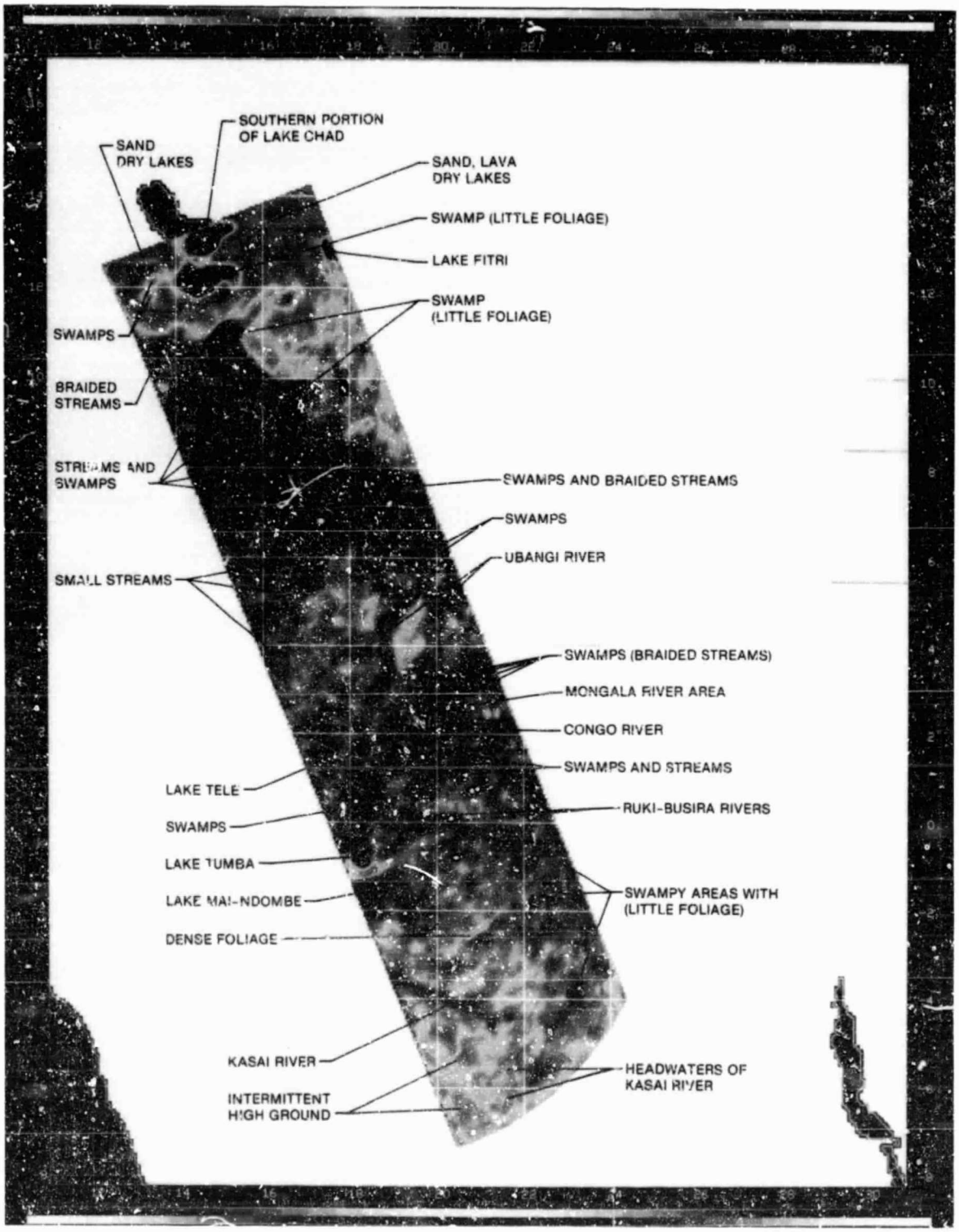


Figure 3-3. The microwave flux image of Figure 3-2 annotated

The areal extent of Lake Mai-Ndombe (Lac Ndombe) appears to be much larger than what would be expected from an inspection of a visible image or a map. The reason the lake appears larger is because visible images and maps deal only with the size of the lake to the foliage line surrounding the lake. Per contra, microwave flux penetrates foliage and shows the surface water that stands in streams and pools below the foliage canopy. It is not uncommon for tree roots to be submerged below the water line on and beyond the perimeter of the tree line that surrounds a lake.

The Ruki and Busira Rivers are formed in a pattern similar to that of the Kasai, from watershed areas and braided streams. The blue-green shades that form the main bore of the Ruki and Busira show that standing water extends well into their foliated sides.

Lake Tele is shown at 1.5° N lat./17.3° E long., near the western edge of the image. When photographed in the visible or infrared, Lake Tele appears to be pear- or oval-shaped because this is the visible pattern of the foliage line around the lake. Lake Tele has a visible diameter of about 4 kilometers. The shape of the lake is different for visible or infrared and for microwaves because of the relative foliage penetration capability of the sensors. Lake Tele has been photographed in situ and is shown in Figure 3-4. The photograph shows the highly reflective properties of the surface of the lake as it mirrors the persisting cloud scene above.

An extensive pattern of standing pools of water and braided streams is shown near 5° N lat./16° E long. These seem to be channeled into the large open swamp area (7° N lat./18° E long.) near the eastern perimeter of the image.

The northern portion of the image shows large areas of open swamps. These may, in fact, be lightly covered by foliage, grasses, and wood debris that are easily penetrated by microwaves.

Figure 3-4. Lake Tele, a mirror in the rain forest. The camera captures the cloudforms and their reflection in the lake. The visible perimeter of the tree line around the lake and the horizon merge as one. (Photograph courtesy of the Unicorne Research Foundation)

Lake Fitri is seen in shades of blue and green near 13° N lat./17.5° E long., on the eastern edge of the image. The lake is serviced by streams and watershed areas to the east. The water level varies greatly with the abundance or scarcity of rainfall in the region.

A large open swamp area is seen at 12° N lat./15° E long., south of Lake Chad. The swamps, and the areal extent of the water they contain, change seasonally with the amount of rainfall.

The southern portion of Lake Chad is seen in shades of blue at 13° N lat./ 15° E long. The water level varies considerably in Lake Chad throughout the year, and when it drops, large areas of exposed mud and sand result. Dry mud and sand appear in shades of red in the microwave flux image.

The microwave flux penetrates surface materials such as sand, soil, dry mud, dry lakes, and lava fields to the extent of a few centimeters in depth. Frequently this capability is useful to identify and map the areal extent of liquid water reservoirs that are near, but below, the surface.

The red shades near the top of the image signify the occurrence of dry lakes, lava beds, and sand that abound on the southern perimeter of the Sahara near Lake Chad.

## D. OBSERVING CONDITIONS

The image of the Congo Basin and its surroundings has been produced as a color rendering from data taken from the public archive for the passive microwave sensor on the SEASAT spacecraft.

The satellite overpass occurred during daylight at 0707 hours UT on August 21, 1978. Dense (non-raining) cloudforms obscured the basin area during the time of the overpass (see Figure 3-5). There is no evidence of precipitation within the extent of the image.


Figure 3-5. A visible wavelength image of the Congo Basin. Prominently displayed in the center of this visible image is the elongated form of Lake Tanganyika lying north to south. Of similar shape is Lake Malawi, southeast of Lake Tanganyika. Lake Victoria is covered with clouds over most of its areal extent and is slightly to the northeast of the northern tip of Lake Tanganyika. The southeastern extent of the Congo Basin, in Zaire, is shown covered with dense cloudforms. The clouds may be seen in the upper left corner of the image. This visible wavelength image was taken within a few hours of the time that the microwave flux imager observed the scene. (Photograph produced from the USAF DMSP film transparencies archived for NOAA/NESDIS at the University of Colorado, CIRES/National Snow and Ice Data Center)

## E. IMAGE GEOMETRY AND TIME

The image is a Mercator projection with width and length dimensions of 603 and 1290 km, respectively, and an areal extent of 770,000 square kilometers.

The elapsed time for the observation was 4 minutes and 57 seconds.

The image commences in southern Zaire in an ascending node and terminates in Chad.

## F. DETECTION CRITERIA

The detection capability of the microwave sensor, for the emitting objects on the surface, is specified by the flux density (radiant emittance) of a Lambertian Disk Emitter whose diameter is 1600 meters and whose temperature difference, with respect to the earth's background temperature, is 2 kelvins.

The irradiance of the Lambertian Disk Emitter arrives in the wavefront at the collecting aperture after transiting a slant range of 1000 km. The irradiance is sufficient to produce a 10-dB signal-to-noise ratio (S/N). The S/N is referenced to the phase center of the collecting aperture. The noise term, N, in S/N includes the surface clutter components that enter the directional diagram of the collecting aperture and the RMS noise level of the receiver.

The data for the image were collected by an articulating aperture whose surface area is 0.49 m. The observing wavelength was 8 mm.

TECHNICAL REPORT STANDARD TITLE PAGE

| 1. Report No. 85-21 | 2. Government Accession No. | 3. Recipient's Catalog No. |
|---|---|---|
| 4. Title and Subtitle<br>Microwave Hydrology: A Trilogy | | 5. Report Date<br>April 1, 1985<br>6. Performing Organization Code |
| 7. Author(s) J.M. Stacey, E.J. Johnston, M.A. Girard, and H.A. Regusters | | 8. Performing Organization Report No. |
| 9. Performing Organization Name and Address<br>JET PROPULSION LABORATORY<br>California Institute of Technology<br>4800 Oak Grove Drive<br>Pasadena, California 91109 | | 10. Work Unit No.<br>11. Contract or Grant No.<br>NAS7-918<br>13. Type of Report and Period Covered<br>JPL Publication<br>External Report |
| 12. Sponsoring Agency Name and Address<br>NATIONAL AERONAUTICS AND SPACE ADMINISTRATION<br>Washington, D.C. 20546 | | 14. Sponsoring Agency Code<br>RE4 BP-161-10-01-40-00 |

15. Supplementary Notes

16. Abstract

Microwave hydrology, as the term in construed in this trilogy, deals with the investigation of important hydrological features on the Earth's surface as they are remotely, and passively, sensed by orbiting microwave receivers. Microwave wavelengths penetrate coulds, foliage, ground cover, and soil, in varying degrees, and reveal the occurrence of standing liquid water on and beneath the surface.

The manifestation of liquid water appearing on or near the surface is reported by a microwave receiver as a signal with a low flux level, or, equivalently, a cold temperature. Actually, the surface of the liquid water reflects the low flux level from the cosmic background into the input terminals of the receiver.

This trilogy describes and shows by microwave flux images:

(1) The hydrological features that sustain Lake Baykal as an extraordinary freshwater resource.

(2) Manifestations of subsurface water in Iran.

(3) The major water features of the Congo Basin, a rain forest.

| 17. Key Words (Selected by Author(s)) | 18. Distribution Statement |
|---|---|
| Agriculture (General); Electronics and Electrical Engineering; Earth Resources; Hydrology and Limnology | Unclassified; unlimited |

| 19. Security Classif. (of this report) | 20. Security Classif. (of this page) | 21. No. of Pages | 22. Price |
|---|---|---|---|
| Unclassified | Unclassified | | |